Electronic Admittances of Parallel-Plane Electron Tubes at 4000 Megacycles

By SLOAN D. ROBERTSON

This paper reports the results of some measurements of the electronic admittances of close-spaced parallel-plane diodes and "1553" triodes at a frequency of 4060 megacycles. These results reveal that the diode admittance and the input short-circuit admittance of the triode depart considerably from the values predicted by single-velocity theory. The triode transadmittance, however, is only slightly lower in magnitude than the low-frequency value.

THE high-frequency admittances of electron streams flowing between parallel-plane electrodes have stimulated considerable theoretical interest. Llewellyn[1,2,3,5] has given an analysis of the particular case in which all electrons in any plane perpendicular to the direction of flow are assumed to have identical velocities. In practice, this approximation gives a reasonably accurate expression for electron stream admittances if the electrode spacing is relatively large, and if the frequency is not so high that the actual spread in electron velocities represents an appreciable fraction of the transit time. Others have treated various aspects of the general problem[4,5,6,7,8,9,10]. Theoretical consideration has also been given to the problem of electron flow in which the electrons possess a Maxwellian velocity distribution[11,12,13,14]. There has been, however, no complete analysis of the microwave-frequency case which takes account of the Maxwellian velocities.

In order to orient the present work properly with previous work let us consider briefly the parallel plane diode shown in Fig. 1, which shows three representative potential distribution curves. If only a relatively few electrons are available at the cathode, the potential distribution between electrodes will be approximately equal to the space-charge-free distribution indicated by curve *a*. If an ample supply of electrons is provided by the cathode and if all electrons leave the cathode with zero velocity, then the space charge is complete in accordance with Child's law, and the potential distribution follows curve *b*. If, on the other hand, the cathode is capable of supplying an ample supply of electrons, the electrons being emitted with a Maxwellian velocity distribution, the potential distribution will be represented by a curve of the type shown by *c*. The cases shown by curves *a* and *b* can be treated by the Llewellyn analysis. With wide spacings and at lower frequencies the admittances obtained with distributions of the *c* type may be approximated by the results obtained by analysis of distributions of the *b* type. With the very close spacings encountered in the Bell

Laboratories 1553 triode[15] the theoretical analysis no longer represents a valid approximation.

Let us consider curve *c* in greater detail. The fact that electrons are emitted with a Maxwellian velocity distribution, instead of being emitted at zero velocity as in the Child's law or complete space charge case, means that more electrons are introduced in the space between the electrodes than can flow to the anode in accordance with Child's law. The surplus electrons depress the potential in front of the cathode to a value below that of the cathode. This potential minimum is indicated by *Vm* in the figure. Electrons which have insufficient energy to cross this barrier return to the cathode.

In the space between the cathode and the potential minimum, electrons are found traveling with various velocities in both directions. Between the potential minimum and the anode, electrons travel in one direction only,

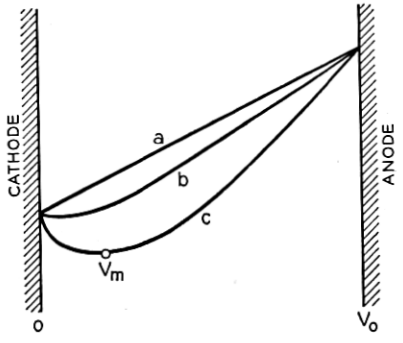

Fig 1—Potential distributions in a diode

toward the anode, but with multiple velocities. With close spacings and higher frequencies the distance between the cathode and the potential minimum may be an appreciable part of the total cathode-anode spacing, with the result that the electrons returning to the cathode may absorb a substantial amount of power from the high-frequency field.

This argument also applies to the cathode-grid region of a microwave triode such as the 1553. In order to increase the transconductance of the triode, it is desirable to locate the grid as close to the cathode as possible. The close spacing, however, leads to a greater loss of power to the returning electrons, which prevents a realization of the full benefits expected from the reduced spacing. All of these difficulties are a result of the Maxwellian velocity distribution of the emitted electrons.

In view of the importance of electron stream admittances in the design of microwave amplifiers and of the need for a better understanding of the performance of the 1553, a program was initiated to investigate some of

these effects experimentally. It seemed best to start this work with a study of the electron stream admittances of simple diodes, with the object of extending the measurements to the triode as the work progressed.

Diodes

The diodes used in this work were identical in construction with the 1553 triode, but for the substitution of a solid copper anode in place of the grid. In all cases the cathode-anode spacing was approximately 0.65 mil, and the area of the cathode was 0.164 square centimeters. With this spacing one would expect the potential minimum to be relatively close to the anode such that a considerable portion of the cathode-anode region would contain electrons moving in both directions. The potential distribution then would be something like that shown in Fig. 2.

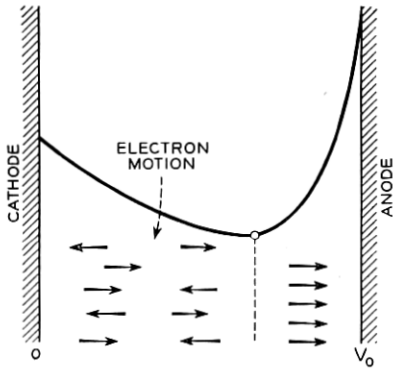

Fig. 2—Electron motion in a close-spaced diode.

The method used in measuring the microwave-frequency input admittances of diodes was based largely on a technique used by Mr. J. A. Morton, and will be described in some detail.

In a typical amplifier, radio-frequency power is fed from a waveguide source to the cathode-grid input region of a 1553 triode through a waveguide-cavity transformer. A similar circuit can be used for measuring diode admittances. The fundamental problem is to learn how to relate admittances measured with a standing wave detector located in the waveguide supply line to the equivalent two-terminal admittances located at the cathode-anode gap of the diode itself. In other words, we have to know the transformation-ratio between an admittance across the cathode-anode gap of the diode and the corresponding admittance which will be measured in the waveguide.

Let us refer to the circuit in Fig. 3. The circuit shows an input trans-

mission line which, for example, may be a waveguide having a characteristic impedance Z_{oy}, connected through an ideal transformer to an output line having a characteristic impedance Z_{ox}. The output line is connected to the transformer at the point x_o, where x_o represents the gap terminals of the diode. Suppose for the moment that provision has been made for connecting the output line at the point in the circuit normally occupied by the cathode-anode planes of the diode. This can be done by means of the special testers shown in Fig. 4. In these testers the anode has been omitted and provision has been made for attaching a coaxial line across the gap between the cathode and anode planes. The diodes used in later tests were identical with the device of Fig. 4, except that the coaxial output fitting was replaced by a sheet copper anode.

Referring again to Fig. 3, assume that the output line is shorted at point x_0. If power is introduced in the input line at the left, a standing wave pattern in the input line will pass through a minimum at some point y_0.

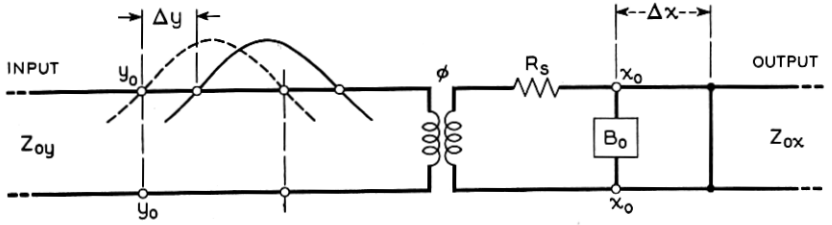

Fig. 3—Equivalent circuit of diode measuring equipment.

If the short circuit is now moved to the right by an increment Δx, the standing wave minimum will move by an increment Δy. The relation between Δx and Δy is given by the following equation:

$$\frac{1}{Z_{0y}} \cot \frac{2\pi\Delta y}{\lambda_y} = \frac{\phi}{Z_{0x}} \cot \frac{2\pi\Delta x}{\lambda_x} - \phi B_0 \tag{1}$$

where λ_y and λ_x are the respective wavelengths in the two lines (which may not be equal if, for example, one is a coaxial and the other is a waveguide). ϕ is the transformation ratio of the ideal transformer, and B_0 is the effective leakage susceptance of the tube and transformer referred to the terminals at x_0. If $\frac{2\pi\Delta y}{\lambda_y}$ is plotted as a function of $\frac{2\pi\Delta x}{\lambda_x}$ on cot-cot coordinate paper, a straight line is obtained whose slope m is

$$m = \phi \frac{Z_{0y}}{Z_{0x}} \tag{2}$$

and whose ordinate intercept ρ is

$$\rho = -\phi B_0 Z_{0y} \tag{3}$$

A typical cot–cot plot is shown in Fig. 5.

Now, assume that the right-hand transmission line is removed and that the diode gap is connected at the transformer terminals x_0. The normalized admittance referred to the point y_0 on the input line can be measured by a simple standing wave measurement. Represent this admittance by $\bar{Y}_{wg}$.

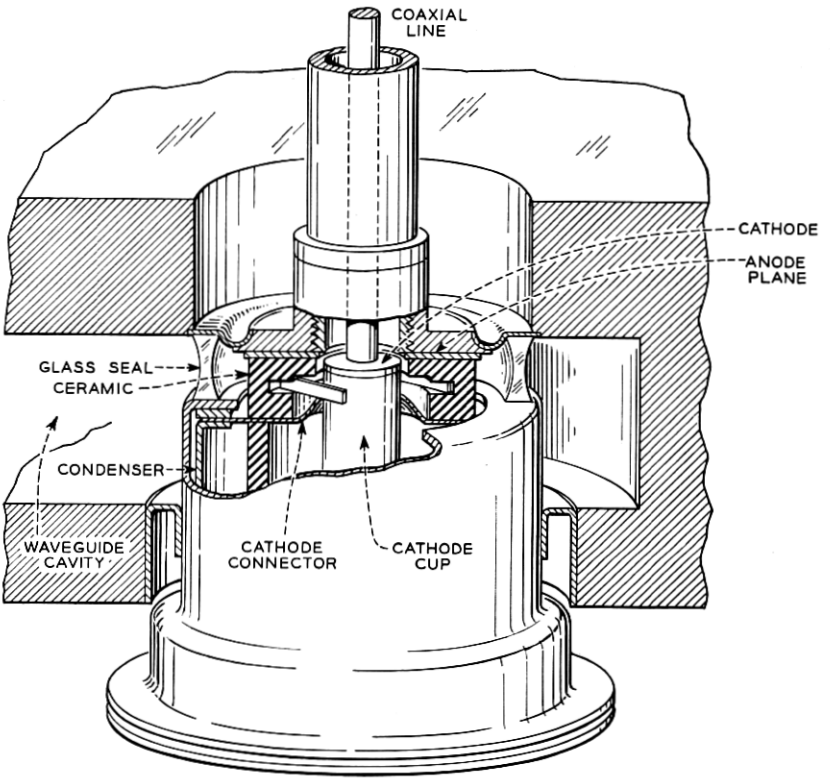

Fig. 4—Coaxial tester.

Let the unknown diode admittance be represented by Y_x. Y_x is then given by the following relation:

$$Y_x = \frac{1}{Z_{0x}m}\left[\bar{Y}_{wg} + j\rho\right] \tag{4}$$

Hence, having determined y_0, it is only necessary to measure the slope m and the intercept ρ on the cot–cot curve in order to relate Y_x to $\bar{Y}_{wg}$. The characteristic impedance of the output line Z_{0x} used in obtaining the cot–cot plot must also be known. Since a coaxial is used for this line, its characteristic impedance is easily calculated.

If no losses were associated with the transformer or the parts of the diode external to the actual cathode-anode region, such as the metal vacuum

envelope and certain ceramic details of the tube, the above measurements would give complete information regarding the circuit. Certain losses have been found, however. These are measured as follows: At the time when terminals x_0 are shorted a standing wave measurement is made in the wave-

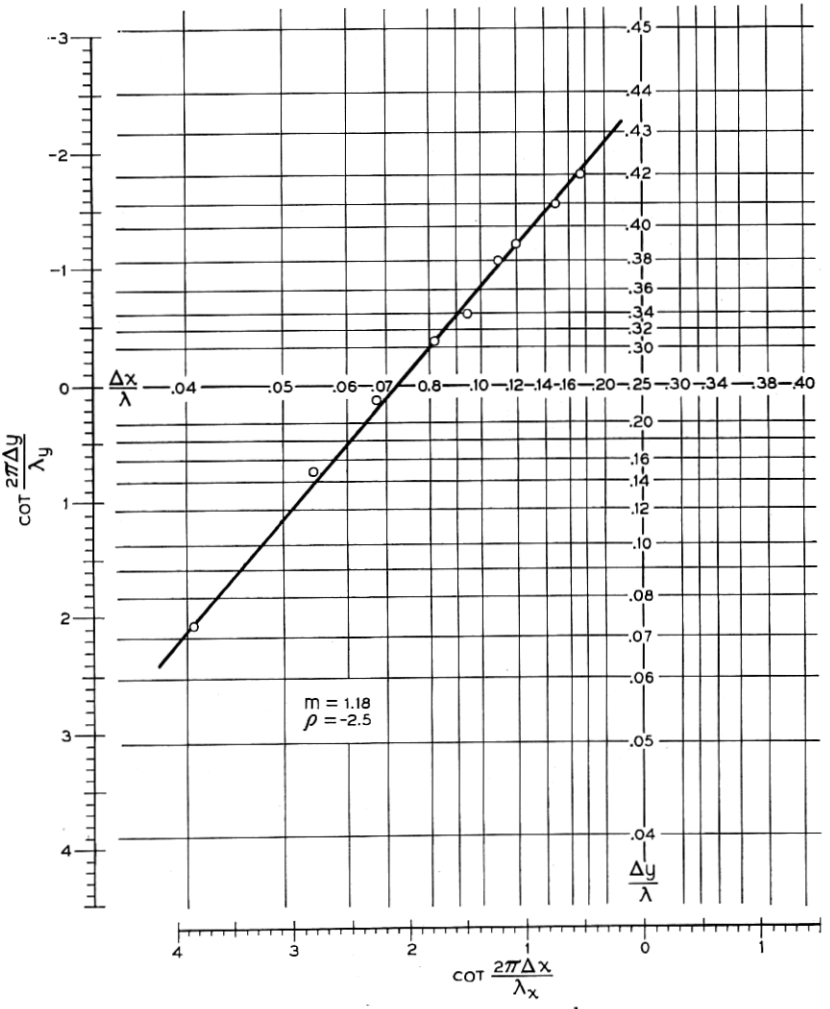

Fig. 5—Typical cotangent–cotangent plot.

guide line at the left. From this measurement and the cot–cot data it is possible to compute an equivalent resistance in series with the gap caused by losses present in the circuit. This equivalent series resistance is given by

$$R_s = \frac{Z_{0x} m}{SWR} \tag{5}$$

where *SWR* is the voltage standing wave ratio mentioned above. The determination of a series loss resistance in this manner is quite analogous to the short-circuit test used in determining the losses in a power transformer.

There is one other factor in the cot–cot technique which is worthy of mention. If, at the very beginning, the output line is terminated in Z_{0x} and if the transformer is adjusted so that the input line is matched, then the value of m will be unity and ρ will equal zero. It is then unnecessary to take a cot–cot curve. It is, however, still necessary to locate y_0 by shorting the terminals at x_0.

Diode Admittance at 4060 Megacycles

Electron stream admittance measurements with diodes were made in the following way: A coaxial tester was installed and the circuit was adjusted for a slope m of about one. This coaxial tester was then removed and replaced by another in order to learn whether the slope obtained with one tester would be the same with another, supposedly identical, tester. This process was repeated several times, and the slope was found to vary no more than about 10% from one tester to the other.

The procedure was then to replace the coaxial tester with a diode and make admittance measurements with the assumption that the slope would be the same for the diode as for the tester. This assumption was believed to be reasonable since the structure of the diode was identical with that of the tester except that an anode was substituted for the coaxial output connector. In either case all elements that were located inside the waveguide cavity were presumably identical.

Electron stream measurements were made at a frequency of 4060 megacycles with a number of diodes over a wide range of anode and heater voltages. In making these measurements, the radio-frequency power was kept at a relatively low level (0.2 milliwatt) in order that the measured admittances would be independent of the radio frequency voltage.

Results for several diodes are shown in Figs. 6 through 13. The various symbols used in the figures are defined as follows:

V_H = heater voltage
I_H = heater current
V_0 = anode voltage (neglecting contact potentials)
I_0 = anode current in ma
J_0 = anode current density in ma/cm^2
g_0 = low-frequency diode conductance measured with an audio frequency bridge
g = high-frequency diode conductance measured as described above
b = high-frequency diode susceptance
R_s = equivalent resistance in series with diode

In computing the admittance of the electron stream it was necessary to

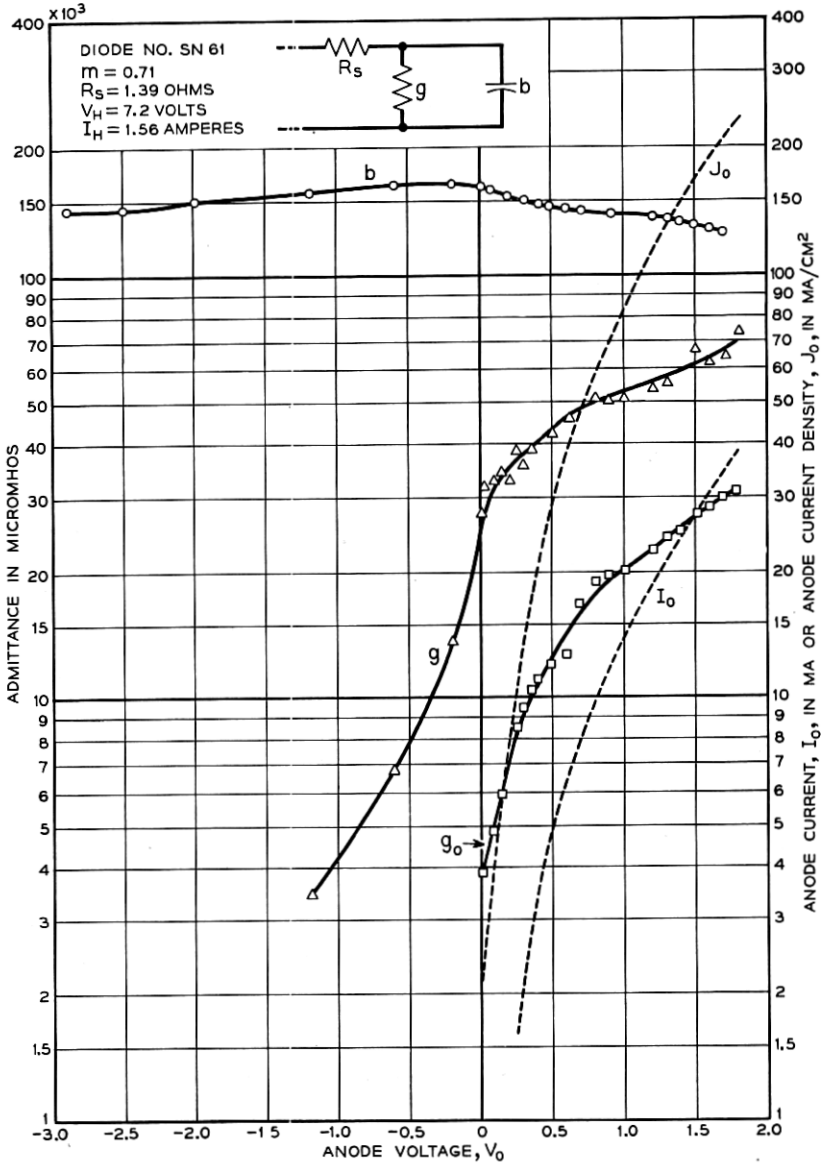

Fig. 6—Admittance of a diode.

allow for the circuit and tube losses previously discussed. The equivalent series resistance R_s of the diode circuit was determined by biasing the tube negatively to the point where a further increase in bias failed to produce a

perceptible change in the waveguide standing wave ratio. Under such conditions the electrons experienced a large retarding field at the cathode and did not emerge an appreciable distance into the cathode-anode region. Any resistance measured at this time was due to the series loss and was not

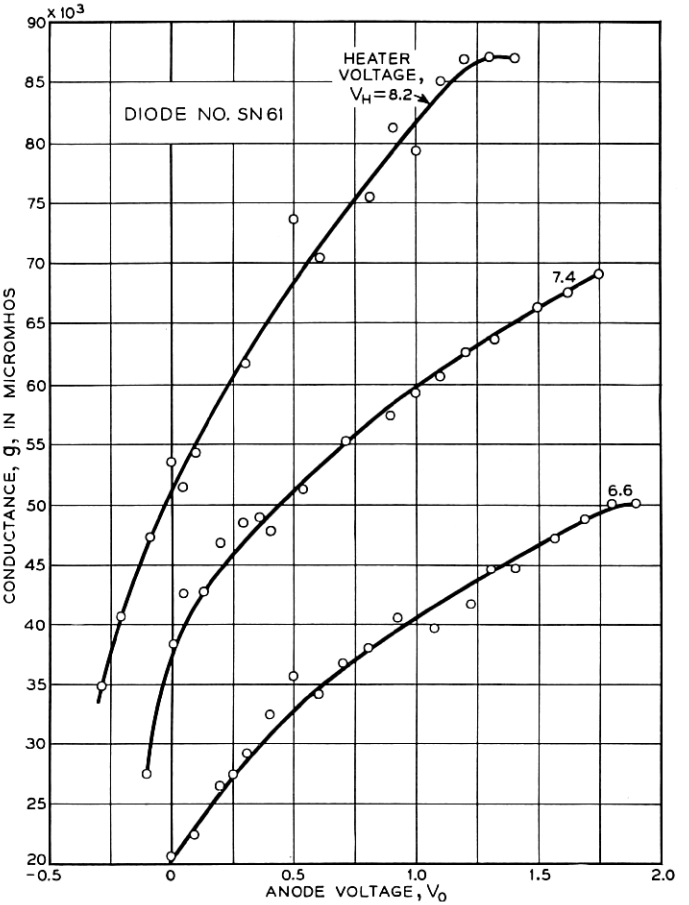

Fig. 7—Effect of heater voltage upon diode conductance.

produced electronically. The diode series resistances varied from about 1.3 to 5.0 ohms with an average value around 3 ohms.

Figure 6 shows the results of admittance measurements of a diode. As expected, the high-frequency conductance is considerably greater than the low-frequency value g_0. In fact g is seen to have a value of several thousand micromhos when the negative bias of the tube is such that no perceptible anode current flows. The susceptance b for large negative anode potentials

has a value of 150,000 micromhos, which agrees fairly well with the value computed from the geometrical capacitance. As anode current is drawn and a space charge condition prevails, b drops to a value of 125,000 micromhos. Theoretical considerations would predict a drop of about 40% in the case of a single-velocity electron stream. This is somewhat greater than the drop exhibited in Fig. 6.

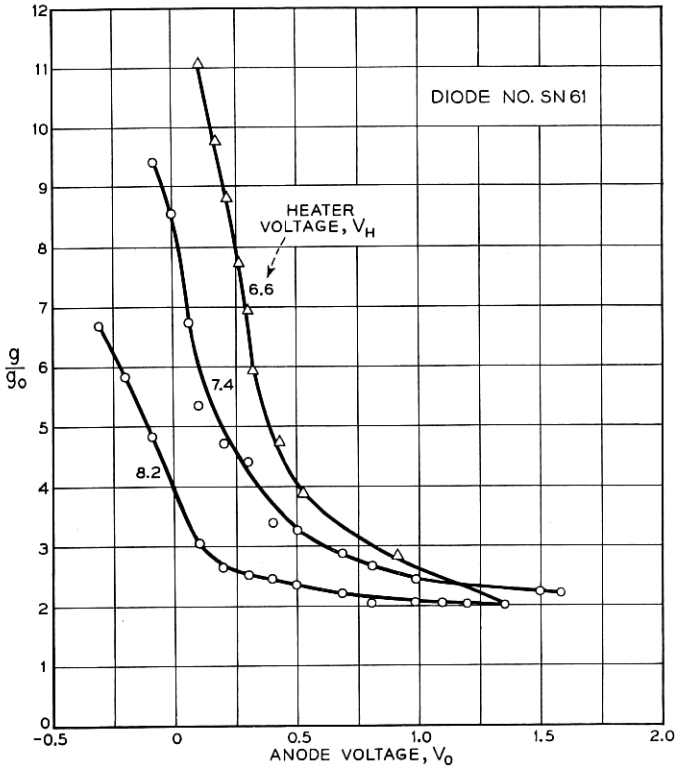

Fig. 8—Effect of heater voltage upon g/g_0.

Figures 7 and 8 show the effect of cathode temperature on g_0 and the ratio g/g_0. The parameter used to represent the cathode temperature is the heater voltage V_H. As the heater voltage is raised the total conductance g increases. The ratio g/g_0, however, decreases, particularly for low or negative anode voltages. This means that, with a given anode voltage, as the cathode temperature is raised, g_0 increases more rapidly than g. If the curves of Fig. 8 are replotted in terms of J_0 rather than V_0, the ratio g/g_0 is relatively independent of V_H. This is shown in Fig. 9.

The results of measurements on another diode are shown in Fig. 10.

These are very similar in all respects to those of the preceding figure. It is probable that the cathode-anode spacings of the two diodes of Figs. 6 and 10 were somewhat greater than the 0.65 mil for which they were designed. In both cases the capacitances measured at low frequency were somewhat low.

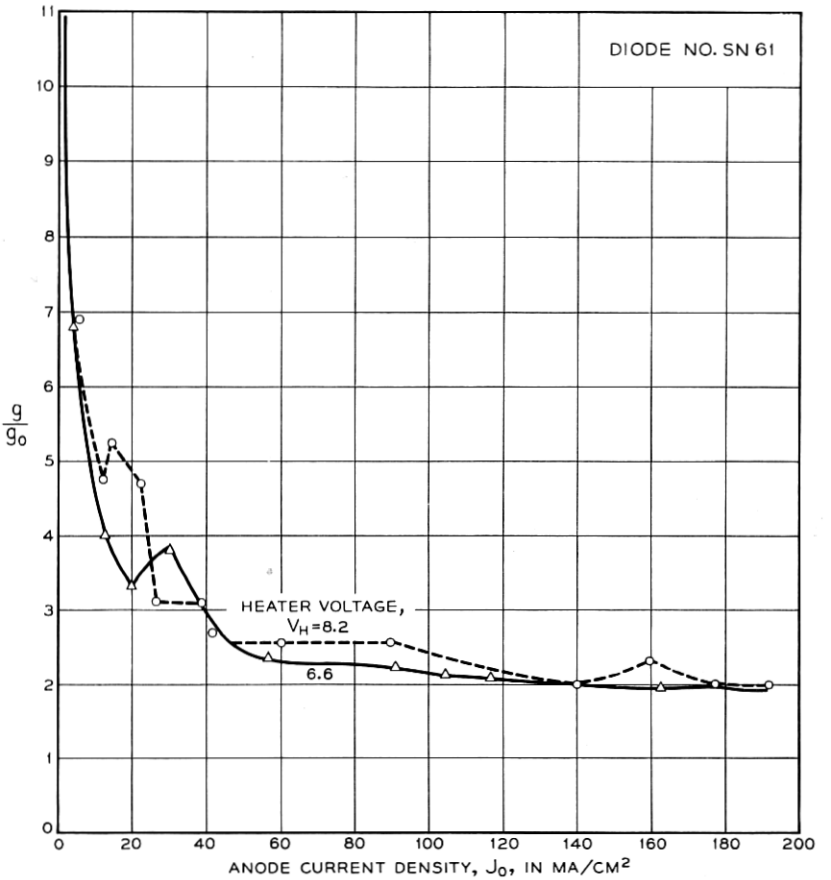

Fig. 9—Variation of g/g_0 with current density and heater voltage.

In Fig. 11, results are shown for a third diode. In this case the susceptance at a large negative bias is in almost exact agreement with the value to be expected with the intended diode spacing of 0.65 mil. It is interesting to observe that, with this tube, b drops a greater amount as the current increases. Moreover, the ratio g/g_0 is greater than that found with earlier diodes.

In Fig. 12 data are shown for a diode having a very high value of g_0. From the standpoint of cathode activity this was the best tube that was

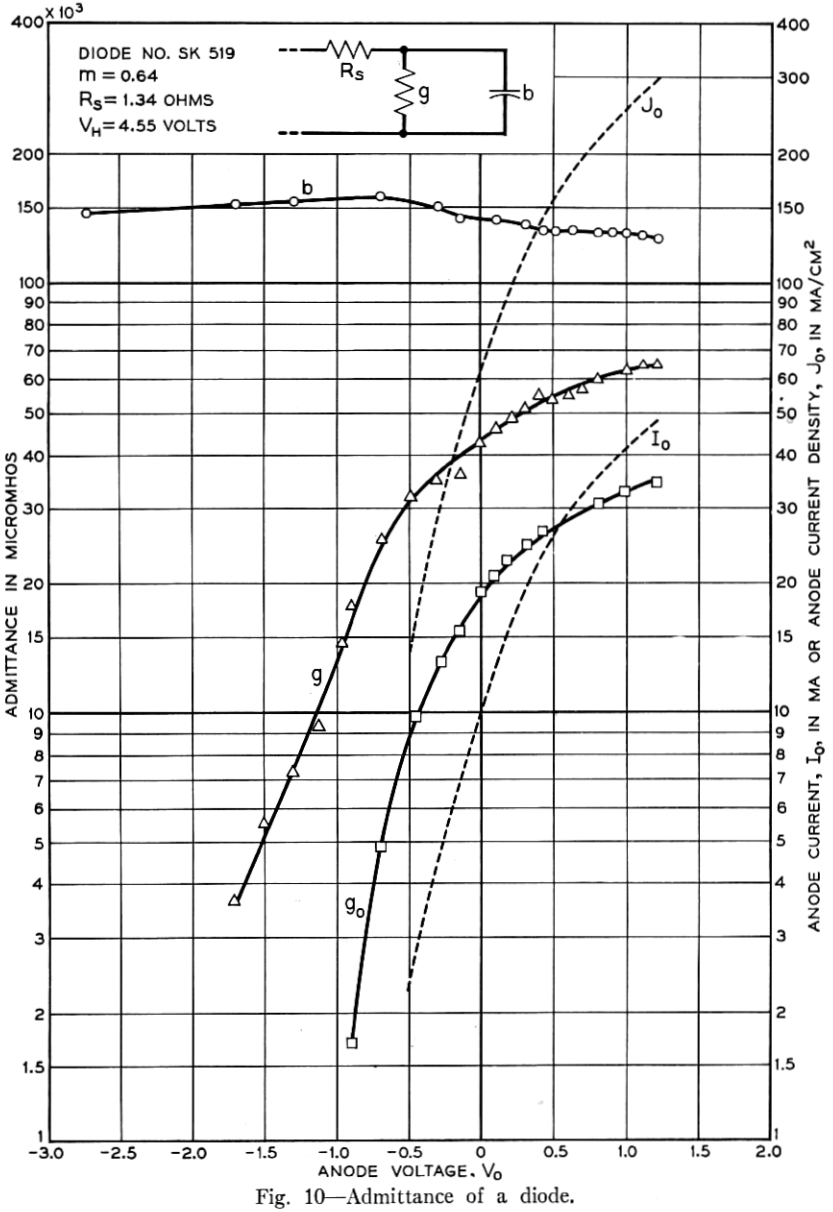

Fig. 10—Admittance of a diode.

tried. At maximum current the susceptance b dropped to 50% of the initial value. The data of Fig. 12 have been replotted in Fig. 13 in terms of the variable $126x^{\frac{4}{3}}/\lambda J_0^{\frac{1}{3}}$, where x is the cathode-anode spacing. In the Llewellyn

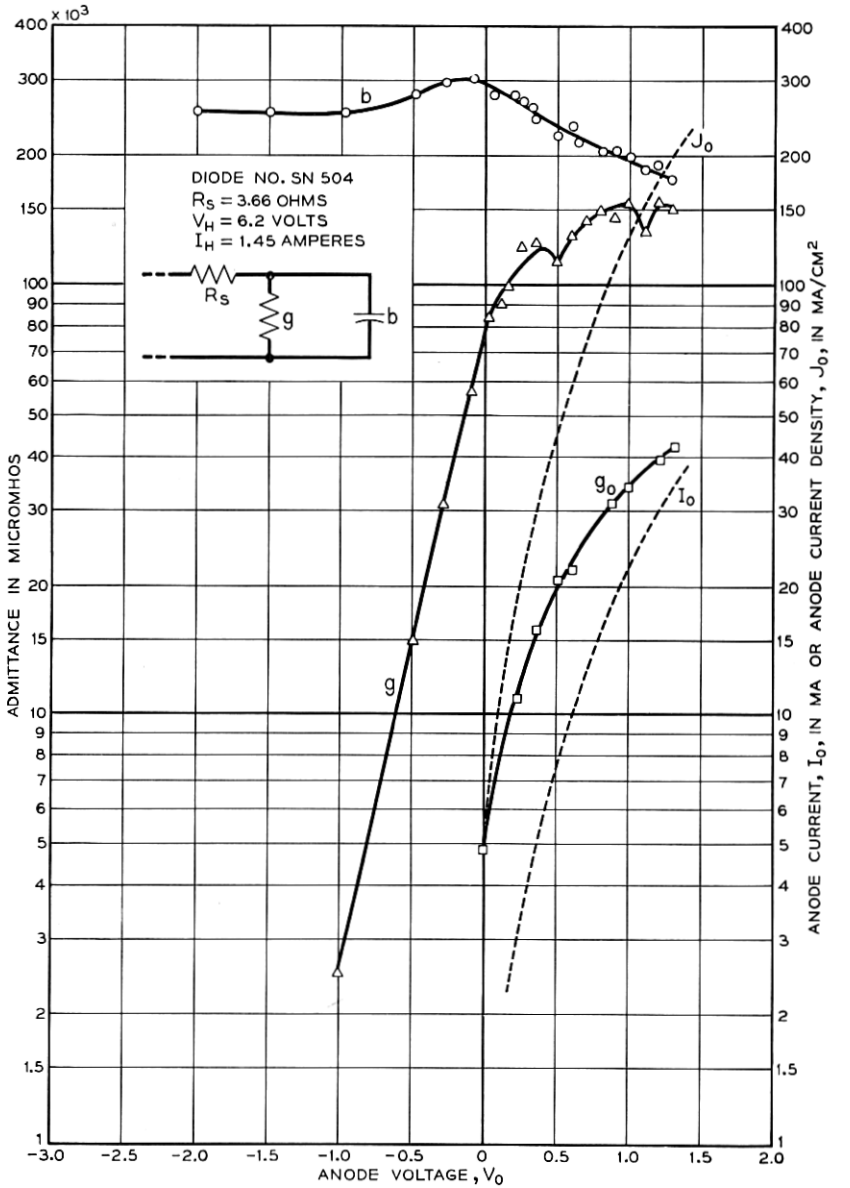

Fig. 11—Admittance of a diode.

theory this variable is equal to the transit time. The solid curves in the figure are the theoretical results of the Llewellyn theory, whereas the broken curves present the corresponding experimental values. In the latter it should

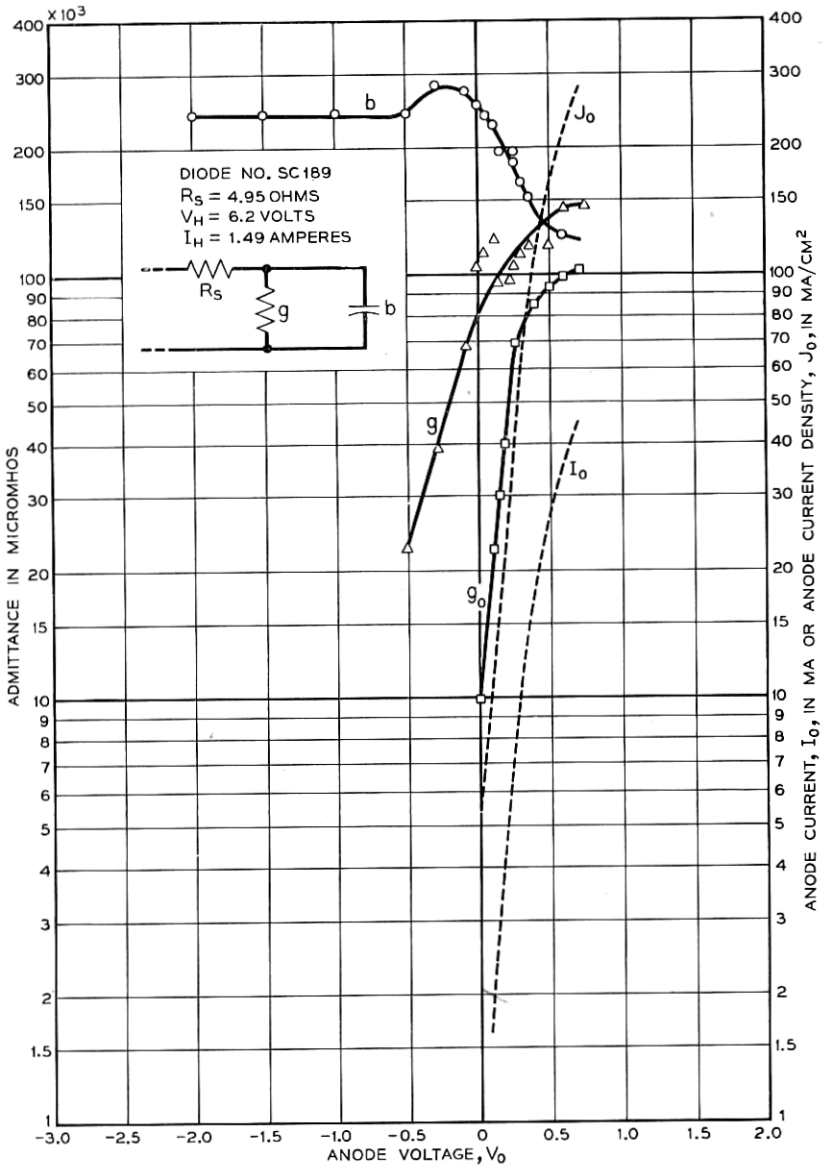

Fig. 12—Admittance of a diode.

be understood that the abscissa do not represent transit time. The curves do serve, however, to compare the theoretical diode resulting from a single-valued electron velocity assumption with the actual diode in which a Max-

wellian velocity distribution prevails. In the experimental case it is probable that, for values of the abscissa greater than 6 or 7, the actual transit time is considerably greater than in the theoretical case. In fact, at a value of 11.4 the anode voltage was zero, the anode current being maintained by the thermal energy of the electrons.

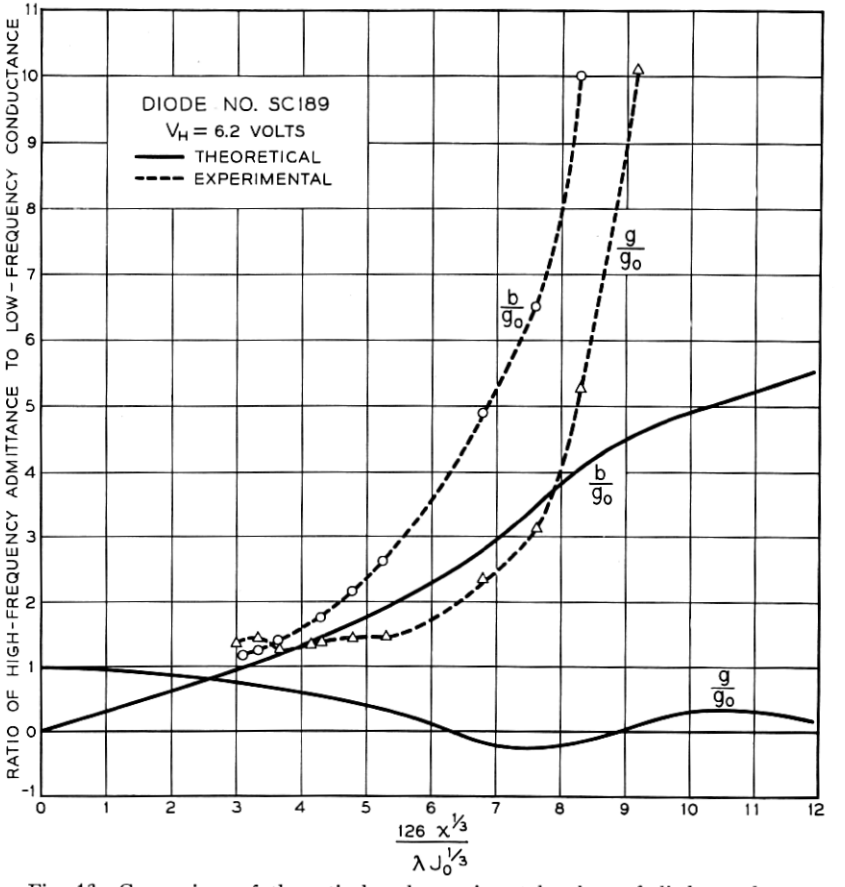

Fig. 13—Comparison of theoretical and experimental values of diode conductance and susceptance.

Other diodes were tested, but they exhibited results substantially equivalent to those already disclosed. In a few cases anomalous results were obtained. With some diodes the capacitance with no electron flow did not approach the low-frequency value. These were rejected on the assumption that there was some mechanical imperfection in the tube which changed the calibration of the measuring equipment.

With the realization that sufficient data are not available to define the phenomena in all detail, it is believed that certain general conclusions can be drawn. From the present work and that of Lavoo[16] and others[17,18,19], it is apparent that the microwave conductance of a close-spaced diode is substantially greater than the low-frequency value. The ratio g/g_0 appears to increase as the spacing decreases. This increase will probably continue until the position of the potential minimum approaches the anode plane. The susceptance decreases with increasing current and appears to level off at high-current densities. The final value at a current density of 240 ma/cm^2 varied between 0.5 and 0.9 of the initial value.

For a given current density, the ratio g/g_0 does not appear to vary appreciably as the cathode temperature is changed.

An attempt was made to study the available diodes at 10,000 megacycles. It was found, however, that the value of R_s was so high at this frequency and that variations in tube conductance were so small in comparison with R_s that accurate results could not be obtained.

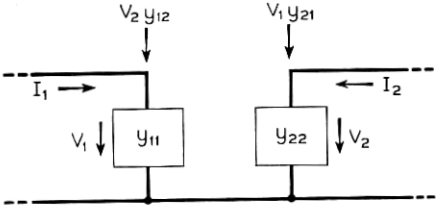

Fig. 14—Equivalent circuit of a triode.

Four-Pole Admittances of a Triode

A triode may be considered as an active linear four-pole transducer, and may be defined by the network of Fig. 14. It is apparent that

y_{11} is the input admittance with the output shorted,

y_{22} is the output admittance with the input shorted,

y_{12} is the feedback admittance with the input shorted,

y_{21} is the transadmittance with the output shorted.

The values of the parameters y_{11}, y_{22}, y_{12}, and y_{21} to be measured at the grid, cathode, and anode terminals differ from the values of the y admittance coefficients given by Llewellyn and Peterson[5] who define y_{11} as the admittance of the diode coinciding with the cathode and the fictitious equivalent grid plane, and y_{22} as the admittance between the equivalent grid plane and the anode, and finally y_{21} as the transadmittance between the two. The relations between the y admittance coefficients of Llewellyn and Peterson and the coefficients measured by the author are given by Peterson.[6] It turns out that, with a high-mu tube, such as the 1553 triode, the two sets of

coefficients differ in the order of 10–20% over the useful operating range of current densities; so, for practical considerations, the measure coefficients may be regarded as substantially equivalent to the coefficients referred to the fictitious grid plane. Not that they will be equal to the theoretical values, but they may be regarded as being associated with the same geometry and will serve at least as a qualitative test of the validity of the theoretical values for the physical tube.

In order to measure the four-pole parameters, the 1553 triode was mounted in a coaxial circuit of the type shown in Fig. 15. The grid-anode output circuit of the tube is seen to connect directly with the coaxial output line. The input circuit required a more careful design. Due to the size of the base of the tube it was necessary to taper the input coaxial as shown. In the early stages of this work, difficulty was experienced with higher order modes in the large diameter section of the input coaxial. It was believed that these modes were generated by the action of the parallel wire grid which lacked the

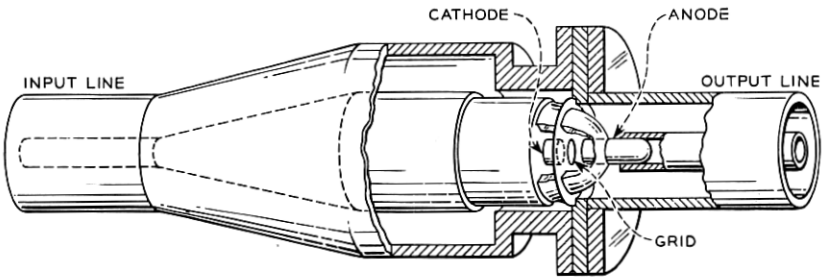

Fig. 15—Detail of coaxial mount for measuring four-pole admittances of a triode.

radial symmetry appropriate to coaxial transmission. The difficulty was overcome by constricting the outer diameter of the coaxial line in the immediate vicinity of the grid of the tube, thus inhibiting generation of the higher order mode.

Before measurements could be made it was necessary first to calibrate both the input and the output circuits in a manner similar to that used and described in connection with the diode measurements. The coaxial tester used for calibrating the input circuit was identical with that used for the diode work. For the output circuit a similar tester was use. As one might expect, the value of the cot–cot slope of the output circuit was close to unity. The value actually turned out to be 0.9. In the input circuit the slope was so great that it was difficult to measure, so that it was necessary to introduce a transformer in the coaxial input circuit to permit tuning.

The complete apparatus necessary to measure y_{11} and y_{22} is shown in Fig. 16. This equipment, save for the details already discussed, is quite conventional in every respect.

In order to measure y_{11}, the output coaxial line was short-circuited at a point an integral number of half-wave-lengths from the grid-anode terminals of the tube. The admittance measured in the input line could then be used in computing y_{11}. To measure y_{22}, the procedure was reversed, the input line being shorted, and the corresponding admittance being measured in the output line. In either case the normalized line admittances were measured by the standard procedure of determining the standing wave ratio in the line and locating the position of the standing wave minimum with respect to the equivalent terminals of the tube.

The transfer admittances were measured with the equipment shown in Fig. 17. The equipment shown here has been fully described in a recent

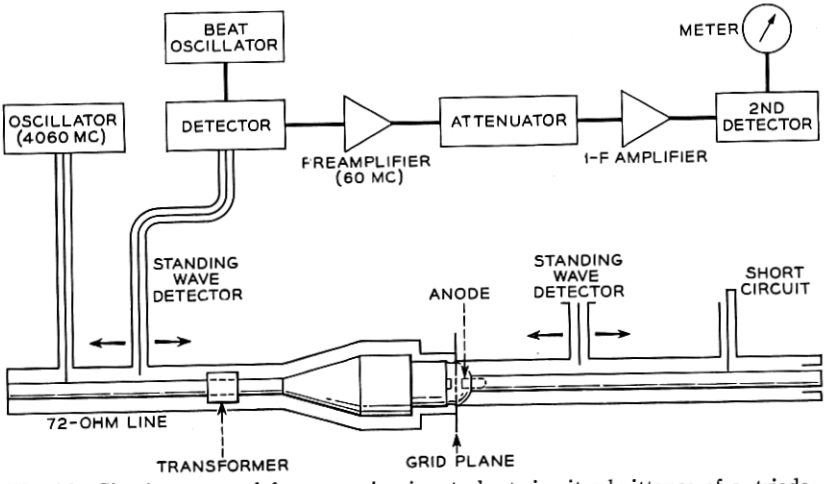

Fig. 16—Circuit connected for measuring input short-circuit admittance of a triode.

paper[20] and will be described only briefly here. The output of a signal oscillator is divided into two portions. One portion is applied to a balanced modulator where it is modulated by an audio-frequency signal. The suppressed-carrier, double-sideband signal from the modulator is applied to the input circuit of the triode. Probes are provided for sampling the voltages V_1'' and V_2'' at points an integral number of half wavelengths from the input and output gaps of the tube respectively. The other portion of the oscillator power is fed through a calibrated phase shifter and is applied to a crystal detector in the manner of a local oscillator of a double-detection receiver. The signal samples at V_1'' and V_2'' are then alternately applied to the crystal detector where they are demodulated by the action of the homodyne carrier. In each case the phase shifter is adjusted so that the audio signal disappears in the detector output. This occurs when the phase of the homodyne carrier

is in quadrature with the signal sidebands. The difference in phase between the two adjustments of the phase shifter is equal to the phase between V_1'' and V_2''. In measuring the transfer phase from V_1'' to V_2'' the output coaxial line is terminated in its characteristic impedance. By reversing this procedure it is possible, of course, to measure the ratio of V_2'' to V_1'' with the input circuit terminated in Z_0. The ratio of the magnitudes of V_1'' and V_2'' may be measured either with the equipment shown in Fig. 17 by adjusting the phase of the homodyne carrier to maximize the signals in each case and

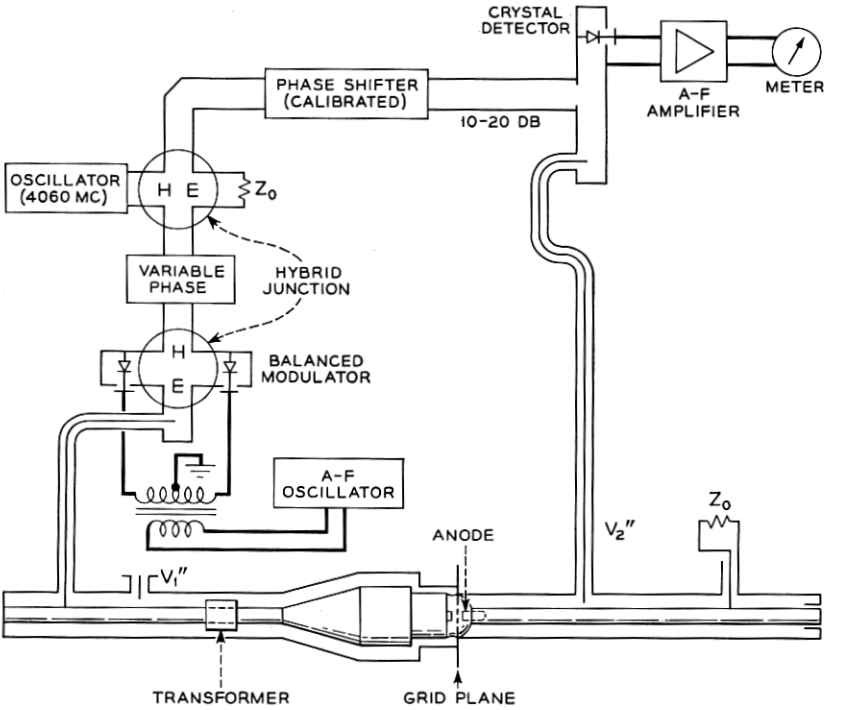

Fig. 17—Circuit for measuring transfer phase of a triode.

comparing the levels, or by using the equipment in Fig. 16 in the conventional way.

Figure 18 is a photograph of the triode circuit which shows the input and output coaxial standing-wave detectors with the triode mounted in the enlarged section at the center.

As in the case of the diode it was found that, with the tube biased negatively such that no electrons could leave the immediate vicinity of the cathode, the input circuit exhibited an equivalent series resistance R_s. The latter had to be allowed for in reducing the experimental data.

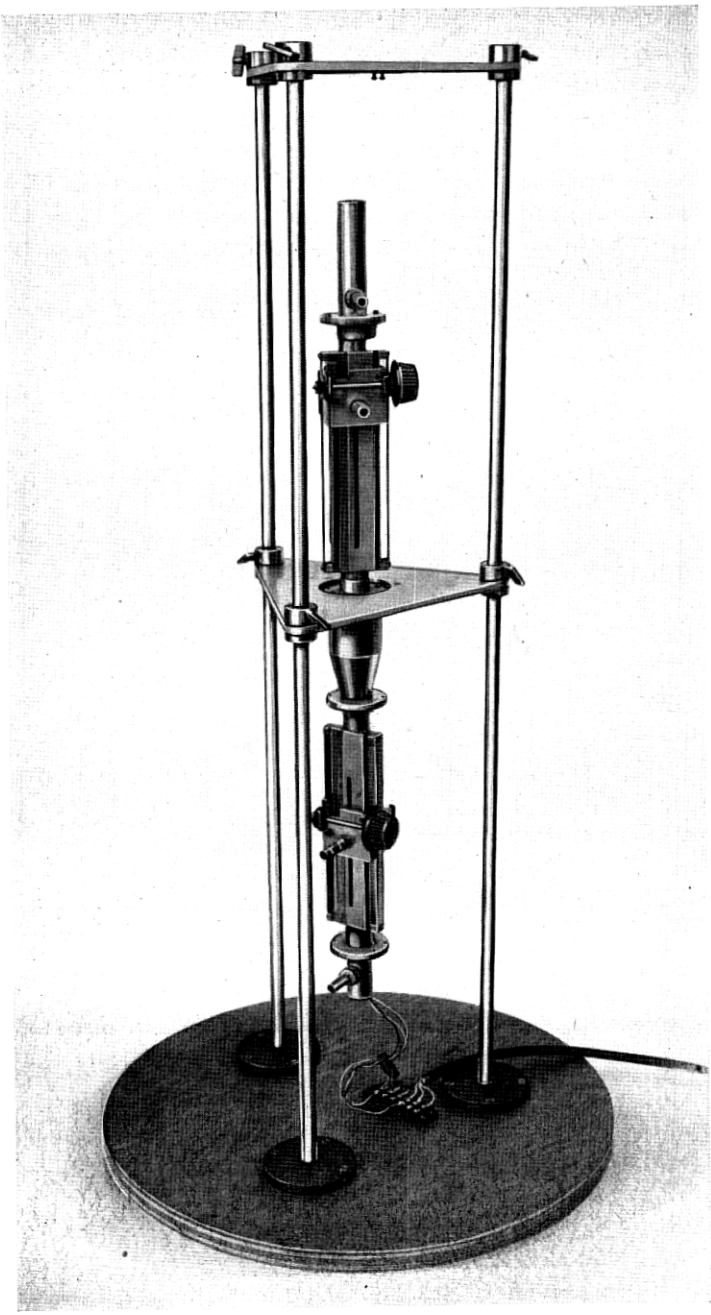

Fig. 18—Coaxial mount for measuring triode admittances.

The experimental data obtained as described above were sufficient for computing the four-pole parameters. The calculations necessary for the reduction of the data can best be understood by referring to Fig. 19. The various symbols used in connection with the figure are defined as follows:

$\bar{Y}_1$ = Normalized admittance measured at 1–1 with 2–2 shorted

$\bar{Y}_2$ = Normalized admittance measured at 2–2 with 1–1 shorted

$\frac{V_1''}{V_2''}$ = γ_{21} (measured with output line terminated in Z_0)

The above parameters represent those obtained by the measurements described above.

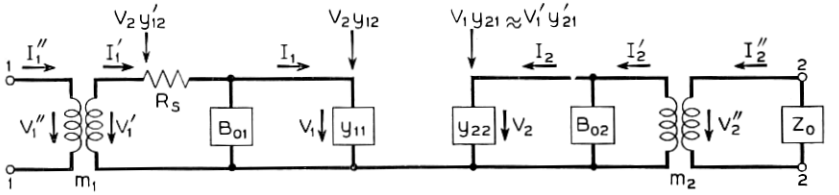

Fig. 19—Equivalent circuit of triode and associated measuring equipment.

In calibrating the circuit the following parameters were obtained:

ρ_1 = ordinate intercept of input cot–cot curve

ρ_2 = ordinate intercept of output cot–cot curve

m_1 = slope of input cot–cot curve

m_2 = slope of output cot–cot curve

$$B_{01} = -\frac{\rho_1}{66m_1} \qquad B_{02} = -\frac{\rho_2}{66m_2}$$

Z_0 = characteristic impedance of input and output coaxial lines.

R_s was measured by shorting the output line, placing a large negative bias on the tube, and measuring the admittance of the input line. Then

$$R_s = 66m_1 Re(\bar{Y}_1) \tag{6}$$

where the number 66 represents the characteristic impedance of the coaxial line used in calibrating the input circuit, corresponding to Z_{0x}: in Equation 4.

Fortunately for simplicity, the series resistance in the output circuit was negligible.

The computations are then as follows:

$$y'_{11} = \frac{\bar{Y}_1}{66m_1} \qquad y'_{22} = \frac{\bar{Y}_2}{66m_2} \tag{7}$$

$$y_{11} = \frac{\bar{Y}_1}{66m_1 - \bar{Y}_1 R_s} + \frac{j\rho_1}{66m_1} \tag{8}$$

$$y_{22} = \frac{1}{66m_2}\,[\bar{Y}_2 + j\rho_2] \tag{9}$$

In order to compute y_{21}, the following four-pole equations are used:

$$V_1' = \frac{I_1'}{y_{11}'} + \frac{V_2 y_{12}'}{y_{11}'} \tag{10}$$

$$V_1 = \frac{I_1}{y_{11}} + \frac{V_2 y_{12}}{y_{11}} \tag{11}$$

$$V_2 = \frac{I_2}{y_{22}} + \frac{V_1 y_{21}}{y_{22}} \approx \frac{I_2}{y_{22}} + \frac{V_1' y_{21}'}{y_{22}} \tag{12}$$

It follows that

$$V_1 y_{21} \approx V_1' y_{21}' \tag{13}$$

$$y_{21} \approx y_{21}' \frac{V_1'}{V_1} \tag{14}$$

Referring to Fig. 19, one may write

$$V_1 = V_1' - (I_1' + V_2 y_{12}')R_s \tag{15}$$

Combining (10) and (15)

$$\frac{V_1'}{V_1} = \frac{1}{1 - y_{11}' R_s} \tag{16}$$

y_{21}' can be evaluated by making use of the relation

$$V_2 \approx \frac{I_2'}{y_{22}'} + \frac{V_1' y_{21}'}{y_{22}'} \tag{17}$$

Dividing (17) by V_2 and rearranging terms

$$y_{21}' \approx \frac{y_{22}'}{\left(\frac{V_1'}{V_2}\right)}\left[1 - \frac{I_2'}{V_2 y_{22}'}\right] \tag{18}$$

where I_2'/V_2 can be expressed as

$$\frac{I_2'}{V_2} = \frac{1}{66m_2\bar{Z}_0} = \frac{1}{66m_2} \tag{19}$$

where $\bar{Z}_0 = 1$.

V_1'/V_2 can be expressed in terms of γ_{21}, m_1, and m_2 by using the relations:

$$\frac{V_1'}{V_1''} = \sqrt{\frac{66m_1}{Z_0}} \qquad \frac{V_2}{V_2''} = \sqrt{\frac{66m_2}{Z_0}} \tag{20}$$

Solving (20) for V_1'/V_2 and remembering that $V_1''/V_2'' = \gamma_{21}$,

$$\frac{V_1'}{V_2} = \gamma_{21}\sqrt{\frac{m_1}{m_2}} \tag{21}$$

If (19) and (21) are substituted in (18), one finds

$$y_{21}' \approx \frac{y_{22}'}{\gamma_{21}}\sqrt{\frac{m_2}{m_1}}\left[1 + \frac{1}{66m_2 y_{22}'}\right] \tag{22}$$

By using (14) and (16), y_{21} can then be written as

$$y_{21} \approx \frac{y_{22}'}{\gamma_{21}}\sqrt{\frac{m_2}{m_1}}\left[1 + \frac{1}{66m_2 y_{22}'}\right]\left[\frac{1}{1 - y_{11}' R_s}\right] \tag{23}$$

Several 1553 triodes were available for study. Typical experimental results obtained with two of them are shown in Figs. 20, 21, and 22. The triode used in obtaining the data of Fig. 20 had input and output spacings of 0.65 and 12 mils, respectively. The cathode and anode diameters were 180 mils. The grid opening was 250 mils and was wound with 0.3 mil tungsten wire at 1000 strands per inch. In the figures, V_g and V_p represent the d-c. grid and plate potentials, respectively.

There are a number of interesting things to observe in Fig. 20. As with the diode, b_{11} for a large negative bias approaches the "cold" value computed from the capacitance. However, as anode current is drawn, b_{11} drops rapidly to a much lower value than was the case for the diodes. The conductance g_{11} behaves somewhat like g for the diode. b_{22} is equal to the value computed from the grid-anode capacitance and is not appreciably influenced by the electron stream. g_{22} was very low with a magnitude of slightly less than 1000 micromhos at maximum anode current. It is not shown in the figure. The transadmittance y_{21} is worth considering. When the bias is several volts negative, y_{21} has a value of about 9000 micromhos. This is about 50 times as high as one would expect from a consideration of the electrostatic capacitance between the cathode and anode of the tube. This effect has been investigated more fully and is discussed in another paper.[21] As the tube starts to draw plate current, y_{21} rises and reaches a maximum of about 40,000 micromhos. The low-frequency transconductance was measured and is plotted in the figure. It will be observed that the high-frequency transadmittance is only slightly lower than g_m. This is in agreement with the theories of Llewellyn.[5] The agreement appears reasonable when one remembers that, in the theoretical analysis, the magnitude of the ratio y_{21}/g_0 is relatively independent of the transit time in the input space.

Figure 21 shows the results of measurements on a triode identical with that of Fig. 20 except that the grid consists of a mesh of 0.3 mil tungsten wires wound at 550 strands per inch in both directions. It will be noted

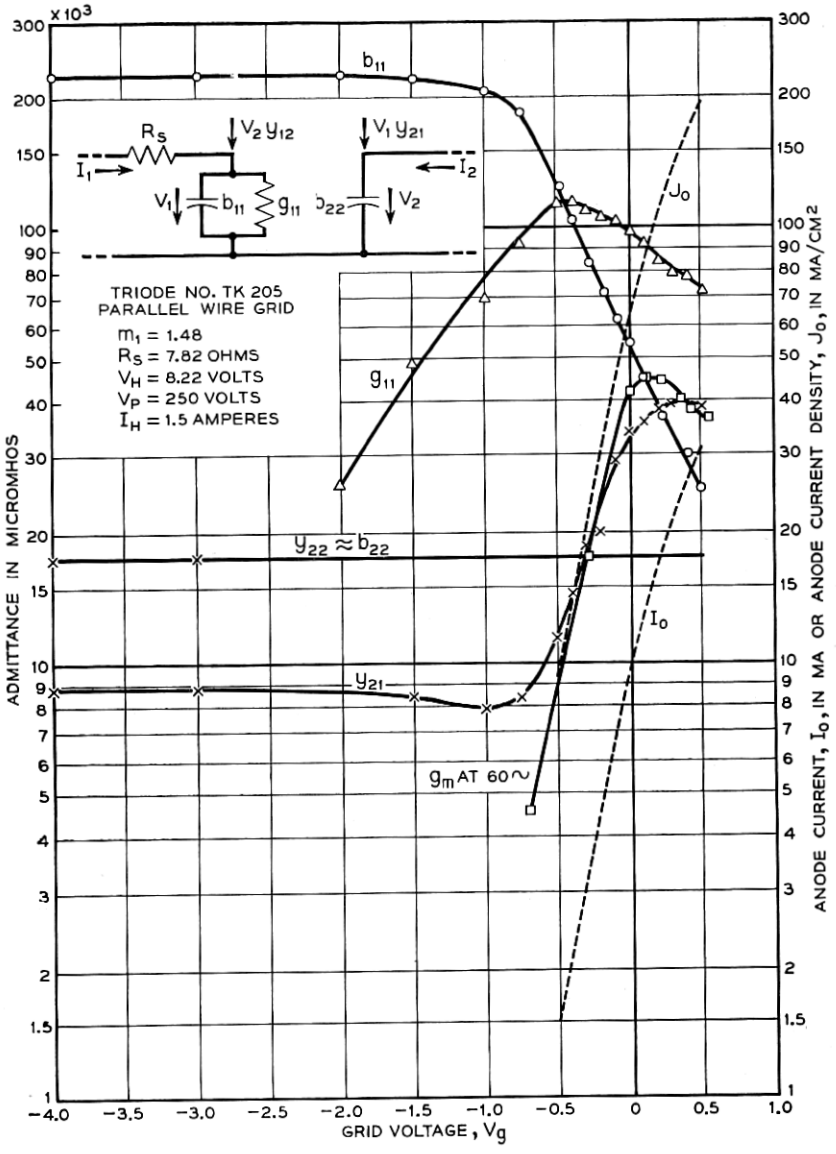

Fig. 20—Four-pole admittances of a triode having a parallel-wire grid.

that y_{21} is much lower when this tube is biased beyond cutoff than in the previous case. The electromagnetic coupling is therefore much less for the mesh grid. This has also been treated in the above reference.[21] With high negative bias the feedback admittance y_{12} was substantially equal to y_{21}

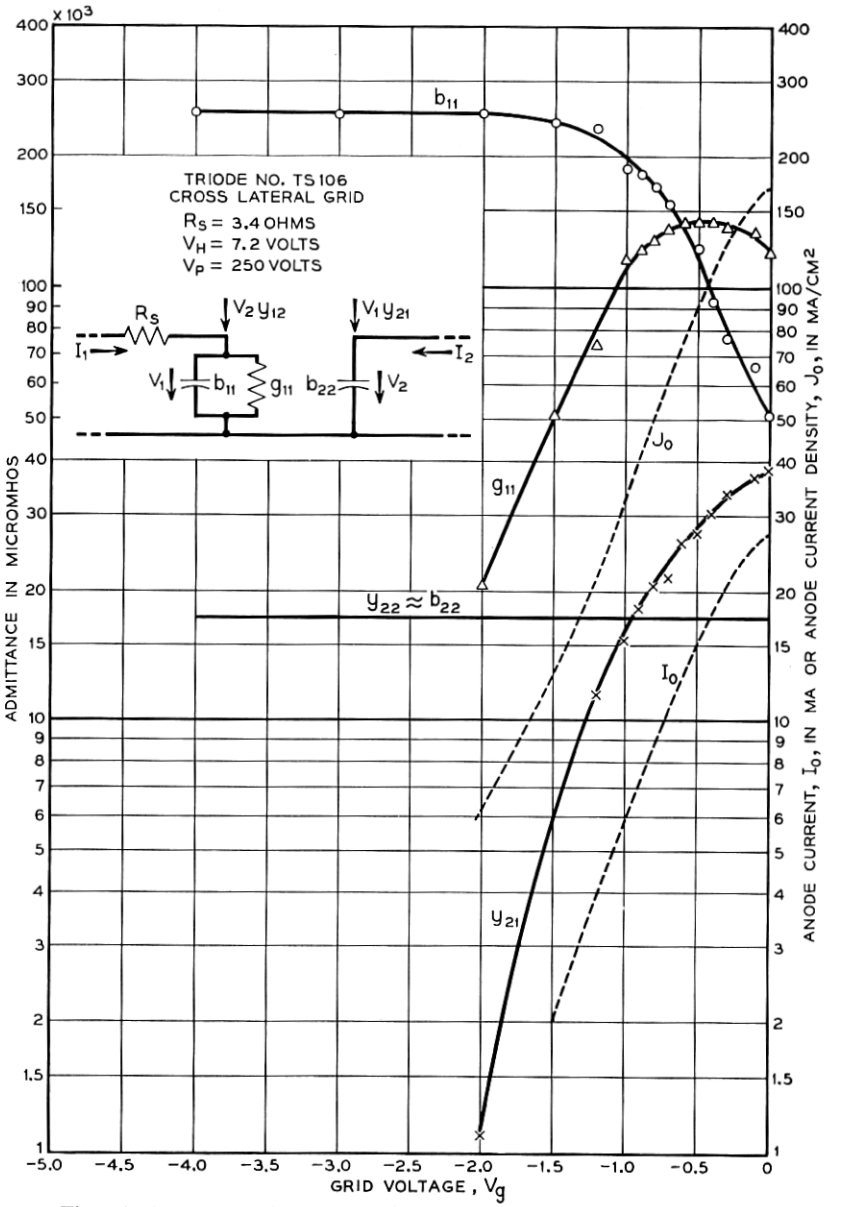

Fig. 21—Four-pole admittances of a triode having a cross-lateral grid.

but, as the current density increased, y_{12} tended to decrease. The feedback admittance was always lower for the mesh grid than for the parallel-wire grid.

The remaining parameters for the triode of Fig. 21 are very similar to those of Fig. 20.

Figure 22 shows the variation of the phase of the transadmittances y_{21} for the two triodes. The figure also shows the theoretical curve of the Llewellyn analysis for purposes of comparison. As in the case of Fig. 13 the abscissa do not represent transit time for the experimental values. The quantity x is equal to the cathode-grid spacing.

It is of interest to compare the triode measurements with those of the diode. It was expected that g_{11} for the triode should correspond with g for the diode. Within the limits of reasonable experimental accuracy this appears to be the case. For the triode at low frequencies $g_0 \approx g_m$. The triode

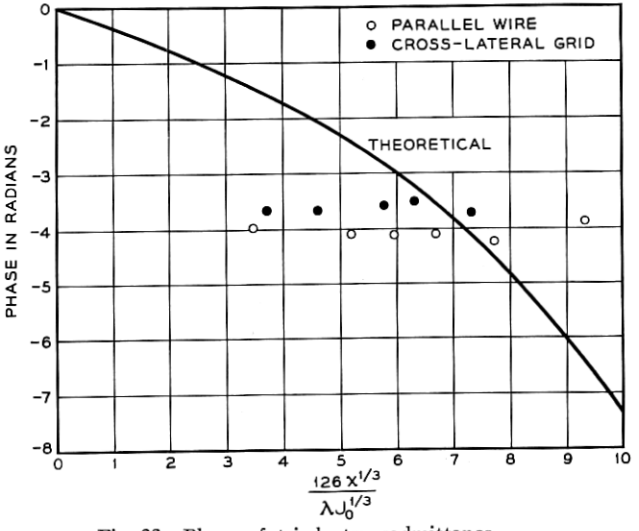

Fig. 22—Phase of triode transadmittance.

results indicate that the ratio g_{11}/g_m is quite comparable in magnitude with the corresponding ratio g/g_0 for the diode. This was expected. The behavior of b_{11} for the triode was unexpected. It was thought that, as the grid voltage was varied so that the input space changed from a condition of zero space charge to one of maximum space charge, b_{11} would vary from its initial "cold" value to a value approaching 60% of the latter. This was not so. In the figures one observes that it drops to a much lower value. This effect has not been explained from a theoretical standpoint. There are several qualitative interpretations, but as yet no way of determining which of them is correct in a quantitative sense has been found. The observed phenomenon could, for example, be explained by an increase in the effective series resistance of the tube caused perhaps by an increase in the resistance of the

cathode coating.[14] Since the effect was not observed to such a marked degree in the case of the diodes, it seems probable that this is not the correct explanation.

It is probable that the observed variation in b_{11} is a space charge effect. It is evident in examining the diode curves that tubes which possessed the higher values for g_0 exhibited a greater variation in b. If maximum g_0 can be taken as a measure of the cathode activity, we can then perhaps relate the variation in susceptance with cathode activity and hence with the location of the potential minimum. A shift in the position of the potential minimum, however, may produce two effects. It varies the transit time of the electrons and changes the degree of space charge in the input space. Either effect might account for the variation of b_{11}. A clue to this effect might be discovered by making measurements on structures with different cathode-grid spacings.

The following experiments were performed to determine the effect of plate voltage on the input admittance of the triode of Fig. 20. The plate and grid voltages were varied simultaneously in such a way that the sum of the direct currents to the grid and plate remained constant at 30 milliamperes corresponding to a current density of 184 ma/cm^2. The input admittance did not vary from the value shown for this same current density in Fig. 20 even though the plate voltage was varied from 250 volts to 40 volts. In a second experiment the plate potential was maintained at -90 volts with respect to the cathode and the grid potential was varied such that the direct grid current varied over a range of 0 to 10 milliamperes. Again the admittances were found to be equal to those of Fig. 20 for the corresponding total currents. These two experiments suggest that, for a given geometry, the value of b_{11} is primarily a function of the total current density in the input circuit.

Acknowledgement

The author wishes to acknowledge his indebtedness to the late Mr. A. E. Bowen who contributed valuable advice during the course of these experiments, to Messrs. J. A. Morton and M. E. Hines who provided the necessary tubes and testers which made this work possible, and to Mr. F. A. Braun who played an indispensable role in the taking and reduction of data.

References

1. "Electron Inertia Effects," F. B. Llewellyn, Cambridge University Press.
2. "Equivalent Networks of Negative Grid Vacuum Tubes at Ultra-High Frequencies," F. B. Llewellyn, *B. S. T. J.*, Vol. 15, pp. 565–586, October 1936.
3. "Operation of Ultra-High Frequency Vacuum Tubes," F. B. Llewellyn, *B. S. T. J.*, Vol. 14, pp. 632–665, October 1935.
4. "Theory of the Internal Action of Thermionic Systems at Moderately High Frequencies," W. E. Benham, *Phil. Mag.*, Vol. 5, pp. 641–662, March 1928; and Vol. 11, pp. 457–517, Feb. 1931.

5. "Vacuum-Tube Networks," F. B. Llewellyn and L. C. Peterson, *Proc. I. R. E.*, Vol. 32, no. 3, pp. 144–166, March 1944.
6. "Equivalent Circuits of Linear Active Four-Terminal Networks," L. C. Peterson, *B. S. T. J.*, Vol. XXVII, No. 4, pp. 593–622, October 1948.
7. "Impedance Properties of Electron Streams," L. C. Peterson, *B. S. T. J.*, Vol. 18, pp. 465–481, July 1939.
8. "Klystron and Microwave Triodes," Hamilton, Knipp and Kuper, pp. 97–169, *Radiation Laboratory Series*, Vol. 7, McGraw-Hill, 1948.
9. "High-Frequency Total Emission Loading in Diodes," Nicholas A. Begovich, *Journal Applied Physics*, Vol. 20, No. 5, pp. 457–461, May 1949.
10. "On the Velocity-Dependent Characteristics of High-Frequency Tubes," Julian K. Knipp, *Journal Applied Physics*, Vol. 20, No. 5, pp. 425–431, May 1949.
11. I. Langmuir, *Phys. Rev.*, 21, pp. 419–435, 1923.
12. "Extension and Application of Langmuirs' Calculations on a Phase Diode with Maxwellian Velocity Distribution of the Electrons," A. Van Der Ziel, *Philips Research Reports*, Vol. 1, No. 2, pp. 97–118, January 1946.
13. "Extension of Langmuir's (ξ, η) Tables for a Plane Diode with a Maxwellian Distribution of the Electrons," P. H. J. A. Klegmen, *Philips Research Reports*, Vol. 1, No. 2, January 1946, pp. 81–96.
14. "Some Characteristics of Diodes with Oxide-Coated Cathodes," W. R. Ferris, *R. C. A. Review*, Vol. X, No. 1, pp. 134–149, March 1949.
15. "A Microwave Triode for Radio Relay," J. A. Morton, *Bell Laboratories Record*, Vol. XXVII, No. 5, May 1949.
16. "Transadmittance and Input Conductance of a Lighthouse Triode at 3000 Megacycles," Norman T. Lavoo, *Proc. I. R. E.*, Vol. 35, No. 11, pp. 1248–1251, November 1947.
17. "Total Emission Damping in Diodes," A. Van Der Ziel, *Nature*, Vol. 159, No. 4046, May 17, 1947, pp. 675–676, (52 mc).
18. "Total Emission Damping," J. Thomson, *Nature*, Vol. 161, No. 4100, pp. 847, May 29, 1948.
19. "Total Emission Damping with Space-Charge Limited Cathodes," C. N. Smyth, *Nature*, 157, 841, June 22, 1946.
20. "A Method of Measuring Phase at Microwave Frequencies," S. D. Robertson, *B. S. T. J.*, Vol. XXVIII, No. 1, pp. 99–103, January 1949.
21. "Passive Four-Pole Admittance of Microwave Triodes," S. D. Robertson, this issue of the *B. S. T. J.*
22. "Total Emission Noise in Diodes," A. Van Der Ziel and A. Versnel, *Nature*, Vol. 159, No. 4045, pp. 640–641, May 10, 1947.
23. "Ultra-High-Frequency Oscillations by Means of Diodes," F. B. Llewellyn and A. E. Bowen, *B. S. T. J.*, Vol. 18, pp. 280–291, April 1939.